Towards predictive cardiovascular safety : a systems pharmacology approach

Snelder, N.

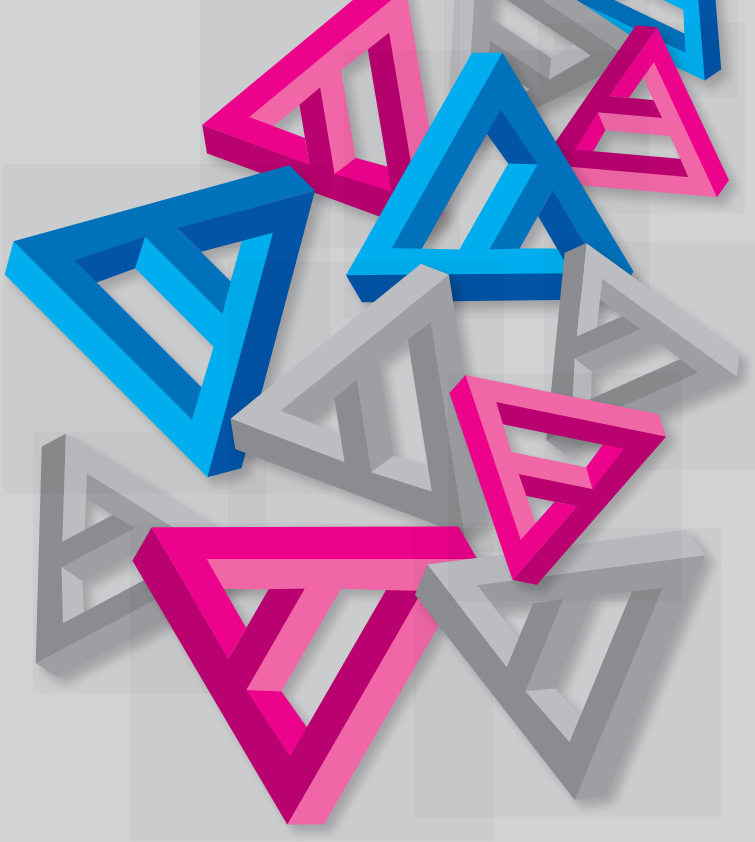

CHAPTER 5

Translational pharmacokinetic modeling of fingolimod as a paradigm compound subject to sphingosine kinase-mediated phosphorylation

N. Snelder, B.A. Ploeger, O. Luttringer, D.R. Stanski and M. Danhof

Drug Metabolism and Disposition; Submitted

Summary

A complicating factor in the translational pharmacology of sphingosine 1-phosphate (S1P) agonists is that they exert their pharmacological effect through their respective phosphate metabolites, which are formed by the enzyme sphingosine kinase (S1PHK). In this investigation, we present a semi-mechanistic pharmacokinetic model for the inter-conversion of S1PHK substrates and their respective phosphates in rats and humans with the aim of investigating whether characterization of the rate of phosphorylation in blood platelets constitutes a basis for interspecies scaling using fingolimod as a paradigm compound. Data on the time course of fingolimod and fingolimod-phosphate (fingolimod-P) blood concentrations following intravenous and oral administration of fingolimod and/or fingolimod-P in rats and following oral administration of fingolimod in doses of 0.5, 1.25 and 5 mg once daily in healthy volunteers were analyzed in conjunction with data on the *ex vivo* inter-conversion and blood-plasma distribution in rat and human blood, respectively. Integrating the data from the *ex vivo* and *in vivo* studies enabled prediction of fingolimod and fingolimod-P concentrations in plasma rather than blood, which are more relevant for predicting drug effects. Large interspecies differences in the rate of phosphorylation between rats and humans were quantified. In human, phosphorylation of fingolimod in the platelets was 4 times slower compared to rat, whereas the de-phosphorylation rates were comparable in both species. This partly explained the 12-fold over-prediction of fingolimod-P exposure in human when applying an allometric scaling approach on the developed rat model. Additionally, differences in pre-systemic phosphorylation should also be taken into account.

Introduction

Fingolimod is a sphingosine 1-phosphate (S1P) receptor modulator, which is effective in the treatment of multiple sclerosis (Cohen *et al.*, 2010). The active metabolite of fingolimod, fingolimod-phosphate (fingolimod-P) binds to 4 of the 5 subtypes of the S1P receptor ($S1P_1$ and $S1P_{3-5}$) with high affinity (0.3-3.1nM) (Mandala *et al.*, 2002; Brinkmann, 2007; Brinkmann *et al.*, 2004; Chun and Hartung, 2010). In contrast, the affinity of fingolimod for all S1P receptors is low (Hale *et al.*, 2004; Albert *et al.*, 2005). The phosphorylation of fingolimod is therefore a critical step in its pharmacological effect. With the discovery of fingolimod and the elucidation of its mechanism of action, the search for other S1P agonists with different pharmacokinetic (PK)-pharmacodynamic (PD) properties has been propelled. Currently available S1P agonists can be categorized into two classes: amino alcohol pro-drugs and second-generation direct agonists (Cusack and Stoffel, 2010). The first class of compounds, to which fingolimod belongs, owes it biological activity to phosphorylation by the enzyme sphingosine kinase (S1PHK) (Billich *et al.*, 2003; Kihara and Igarashi, 2008; Kharel *et al.*, 2005). There are important inter-species differences in the expression and function of S1PHK. In the rat, S1PHK is predominately expressed in the kidney, spleen and liver tissue (Olivera *et al.*, 1998). In humans, S1PHK1, which is one of the two S1PHK isoforms, is mainly expressed in lung and spleen, whereas the other isoform, S1PHK2, is predominantly expressed in liver and heart tissue (Liu *et al.*, 2000; Paugh *et al.*, 2003). These large inter-species differences complicate the prediction of exposure to phosphorylated S1P pro-drugs in humans using *in vivo* animal data. Therefore, an allometric scaling approach, which does not consider inter-species differences in enzyme tissue distribution or enzyme activity, will not be applicable to S1P pro-drugs. Since an adequate characterization of the exposure in rat and human may be important for translational modeling (Danhof *et al.*, 2008) a qualitative and quantitative understanding of differences in the PK of S1PHK substrates between rat and human must be considered.

Fingolimod is an interesting paradigm compound to investigate the pharmacokinetics of S1PHK substrates since the inter-conversion between fingolimod and its phosphate has been well investigated in several *in vitro, in vivo and ex vivo* studies (Albert *et al.*, 2005; Billich *et al.*, 2003; Kihara and Igarashi, 2008; Olivera *et al.*, 1998; Liu *et al.*, 2000; Kovarik *et al.*, 2007). From *ex vivo* studies it is known that fingolimod is phosphorylated in the blood platelets (Albert *et al.*, 2005; Kihara and Igarashi, 2008; Anada *et al.*, 2007). We hypothesize that characterization of the inter-conversion between fingolimod and fingolimod-P in blood platelets may constitute a basis for the scaling of the PK between rats and humans. To date, no PK models have been published that describe the time course of the fingolimod and fingolimod-P concentrations simultaneously. Since the conversion between fingolimod and its phosphate is a reversible and dynamic process it

is anticipated that the PK of fingolimod-P is closely linked to the PK of fingolimod. Therefore, a simultaneous analysis of the *in vivo* concentration-time course of fingolimod and fingolimod-P and the *ex vivo* inter-conversion, and blood-plasma distribution will yield an understanding of the dynamics of the overall inter-conversion and the relevance of the inter-conversion in blood platelets. Moreover, characterizing the blood to plasma distribution allows the prediction of the fingolimod-P plasma concentrations rather than whole blood concentrations, which are the relevant concentrations for the modeling of pharmacodynamic effects in future pharmacokinetic pharmacodynamic investigations.

In this investigation, we present a semi-mechanistic population PK model for the inter-conversion of S1PHK substrates and their respective phosphates using fingolimod as a paradigm compound with the aim a) to investigate whether characterization of the inter-conversion in blood (platelets) constitutes a basis for the scaling of the PK between rats and humans and b) to predict the time course of plasma (rather than whole blood) concentrations of phosphate metabolites.

Materials and Methods

An overview of the studies used to characterize the PK of fingolimod(-P) in rat and human can be found in Table 1.

Ex vivo studies

Three *ex vivo* experiments were performed in isolated blood from male albino rats of strain Hanover Wistar and human blood obtained from healthy male volunteers (Blutspendezentrum SRK, Basel, Switzerland). Experiment A was an inter-conversion experiment in which (rat and human) blood samples (~ 6 mL) were spiked with a fingolimod or fingolimod-P spiking solution (20 µg/mL; solvent: ethanol abs: 1 M HCl (95:5, w:w)) to achieve final concentrations of 100 ng/mL fingolimod and fingolimod-P. In total, 11 samples were incubated at 37°C with gentle agitation. 0.8 mL aliquots were taken after 0, 1, 2, 4, 7, 24 and 48 h of incubation, immediately frozen on dry ice and stored at – 80°C. Fingolimod and fingolimod-P blood concentrations were determined by LC/MS/MS after liquid/liquid extraction. The lower limits of quantification (LOQ) were 1.08 and 2.5 ng/mL for fingolimod and fingolimod-P, respectively. Experiments B and C investigated the blood/plasma distribution of fingolimod-P. In experiment B the time dependency of blood/plasma distribution (time points: 0.25, 0.5, 1, 2 and 4 h) was studied for a concentration of 30 ng/mL [^{14}C]fingolimod-P in rat blood and at 30 and 300 ng/mL [^{14}C]fingolimod-P in human blood. Experiment C investigated the fingolimod-P blood/plasma distribution for the nominal concentrations of 3, 30, 300 and 3000 ng/mL [^{14}C]fingolimod-P in trip-

licate (in addition at 1 and 0.3 ng/mL for human). Samples were incubated for 120 min at 37°C with constant agitation on an orbital shaker. In experiments B and C separation of cells and plasma was achieved by centrifugation (1500 g, 10 min, 37°C). Samples for quantification of total radioactivity were taken before and after (plasma fraction only) centrifugation. The radioactivity in the biological samples was measured by LSC with Irga-Safe Plus (Packard) as Scintillator. Radiometry was performed in TriCarb 2500 TR and 2700 TR Liquid Scintillation Systems (Packard Instr. Co., Meriden, CT, USA). Concentrations of radiolabeled substances in plasma and blood were determined in weighed samples. Data were converted from dpm/g to ng/mL assuming a density of 1.00 g/mL for all samples and using the specific radioactivity.

Studies in rat

The studies in rats were conducted in accordance with the Guide for the Care and Use of Laboratory Animals as adopted and promulgated by the U.S. National Institutes of Health. Study 1, was a single dose PK-PD study in which fingolimod and fingolimod-P concentrations where measured following intravenous (iv) and oral administration of fingolimod, in male, Lewis rats. Rats were provided normal chow and water *ad libitum*. Study 2, was a study on the PK of fingolimod and fingolimod-P after single iv administration of fingolimod or fingolimod-P, in male Sprague Dawley rats (Charles River, France). At the time of study, body weights ranged from 296-318 gram. Rats were provided normal chow (NAFAG pellets No. 890, ECOSAN Eberle NAFAG AG, Gossau, Switzerland) and tap water *ad libitum*. In these pharmacokinetic investigations the vena femoralis was cannulated for compound administration and the arteria femoralis for blood sample collection. Following cannulation, a recovery period of 72 h was observed. Meloxicam was used for post-surgery analgesia (1-2 mg/kg, subcutaneously). Cannulae were filled with aqueous heparin solution. During the recovery time, the functional capability of the cannulae was regularly tested.

Studies in healthy volunteers

The studies in healthy volunteer were conducted in accordance with the Declaration of Helsinki. The protocols for studies 2105, 2213 and 2215 were approved by local medical ethics committees and written informed consent was obtained from all subjects. Subjects were judged eligible for the studies if they were aged between 19 and 50 years or between 18 and 45 years for studies 2105 and 2213/2215, respectively. In addition, all subjects were in good health as determined by past medical history, physical examination, vital signs, electrocardiogram, and laboratory tests at screening.

Table 1: Study overview

Rat					
Study	**Description**	**Dosing regimen**	**Route**	**Blood sample collection**	**Measured**
1	Single dose PKPD study in Lewis rat	Single iv fingolimod dose: 1 mg/kg or single oral fingolimod dose: 0.1, 0.3 , 1 or 3 mg/kg (n=3, per group)	iv and oral	iv: 0, 0.25, 0.5, 1, 2, 6, 24 and 48 h after dose oral: 0, 1, 2, 6, 24, 48, 96, 168, 216, 264 and 336 h after dose	fingolimod and fingolimod-P
2	Pharmacokinetics of fingolimod and fingolimod-P in male Sprague Dawley rats after single intravenous admini-stration of fingolimod or fingolimod-P	Single iv fingolimod dose: 1 mg/kg or single iv fingolimod-P dose: 0.1 mg/kg (n=3, per group)	iv	0.0083, 0.0167, 0.025, 0.033, 0.0833, 0.1667, 0.5 and 1 h after dose	fingolimod and fingolimod-P
Human					
Study	**Description**	**Dosing regimen**	**Route**	**Sampling scheme**	**Measured**
2105	randomized, double-blind, placebo-controlled, multiple dose study in healthy subjects	Once-daily dosing of 0.5 mg fingolimod (n=12), 1.25 mg fingolimod (n=12), or placebo (n=12) for 14 days	oral	Day 1: predose, 1, 2, 6, 8, 12, 16, 20 and 24 h after dose. Days 3 and 7: predose (trough). Days 28 and 42: any time	fingolimod and fingolimod-P
2213	randomized, double-blind, placebo-controlled, multiple dose study in healthy subjects (Kovarik, 2004)	Once-daily dosing of 1.25 mg fingolimod (n=20), 5 mg fingolimod (n=20), or placebo (n=20) for 7 days	oral	Days 1 and 7: predose, 1, 2, 6, 8, 12, 16, 20 and 24 h after dose. Days 2 to 6: before (trough) and 6-8 h (peak) after the daily dose	fingolimod
2215	randomized, single-blind, placebo-controlled, time-lagged, ascending single dose study in healthy subjects	Single dose of 5, 7.5, 10, 15, 25 or 40 or mg fingolimod (n=6, per group) or placebo (n=2, per group)	oral	predose, 0.25, 0.5 1, 1.5, 2, 3, 4, 6, 8, 12, 24, 36 48, 72, 96, (120), 168, 264, 600 and 936 h after the first dose	fingolimod and fingolimod-P

Bioanalytics

Venous blood samples were collected according to the sampling schemes described in Table 1. Blood concentrations were determined by a validated liquid chromatography method with mass spectrometry detection. Samples were analyzed following liquid-liquid extraction (Kovarik *et al.*, 2004). In the studies in rats, the LOQ's were 0.250 and 1 ng/mL for fingolimod and fingolimod-P, respectively. In the clinical studies the LOQ was 0.080 ng/mL for fingolimod. For fingolimod-P, the LOQ's were and 0.1 and1 ng/mL in studies 2105 and 2215, respectively. Assay accuracy ranged from 97.5% to 108.7% and precision coefficients of variation from -2.5% to 8.7%.

Population PK modeling strategy

Two PK models were developed, i.e. one model to characterize the PK of fingolimod en fingolimod-P in rat and one model to characterize the PK of fingolimod and fingolimod -P in human. The rat PK model was developed using data from studies 1 and 2 and the *ex vivo* studies in rat blood. The human PK model was developed using data from studies 2105 and 2213 and the *ex vivo* studies in human blood. Data from study 2215 were used for (external) evaluation of the predictive value of the model.

Only physiologically plausible models were evaluated, i.e. all evaluated models were based on the knowledge from published *in vitro*, *in vivo* and *ex vivo* studies. Briefly, the following is known about the inter-conversion between fingolimod and its phosphate.

i) Fingolimod is phosphorylated peripherally (Olivera *et al.*, 1998; Liu *et al.*, 2000), in the platelets in blood (Albert *et al.*, 2005), and pre-systemically during first-pass in the liver upon oral administration (Kovarik *et al.*, 2007).
ii) Fingolimod-P is dephosphorylated back to fingolimod before it is eliminated from the body (Zollinger *et al.*, 2011).
iii) Dephosphorylation occurs only in the plasma. Fingolimod-P is dephosphorylated by the enzyme lipid phosphatase type 3 (LLP3)(Kihara and Igarashi, 2008), which is expressed in the plasma membrane on cells exposed to plasma such as vascular endothelial cells and blood cells (Kihara and Igarashi, 2008).

One-, two- and three-compartmental models were evaluated to describe the disposition of fingolimod and fingolimod-P. Furthermore, it was investigated if the absorption from the gastrointestinal-tract (dose compartment) to the blood (central compartment) could be described with first- or zero-order processes. In addition, an exploratory graphical analysis of the dose-normalized raw fingolimod and fingolimod-P blood concentrations indicated that absorption, distribution and/or inter-conversion might be non-linear with

dose/concentration. Therefore, it was evaluated if the description of the data could be improved by describing the absorption, distribution or inter-conversion by saturable processes, i.e. by Michaelis-Menten like processes (Equation 1) or by saturable binding to plasma proteins (Equation. 2).

$$SPK = A(x) * \frac{Vm}{Km + C(x)} \quad (1)$$

In this equation A(x) is the amount in compartment x, C(x) is the concentration in compartment x, *Vm* is the maximum rate of biotransformation and *Km* is the concentration at which the half maximal rate of biotransformation is reached. The term SPK is used to represent saturation of a certain mechanism, e.g. a saturable distribution or saturable inter-conversion. It results in a sigmoid relationship approaching a maximum at infinitely high concentration.

$$phi = \frac{(C - B_{max} - Kd) + \sqrt{(C - B_{max} - Kd)^2 + 4 * Kd * C}}{2 * C} \quad (2)$$

In case of saturable binding, in this equation, phi is the free fraction, C is the total concentration in the plasma and B_{max} and *Kd* are the binding capacity and binding affinity, respectively.

Allometric scaling

The PK of fingolimod and fingolimod-P in human was also predicted from the rat model using an allometric scaling approach (West *et al.*, 1999). This approach describes how biological properties vary with body mass. As the fingolimod and fingolimod-P plasma protein binding is comparable for rat and human, predictions were not corrected for differences in the unbound fraction. Mean body weights of human and rat were assumed to be 70 and 0.3 kg, respectively. All rate constants were scaled with an allometric exponent of - 0.25 and an exponent of 1 was used for scaling the volume of distribution. The absorption was not scaled, according to the assumption that the bioavailability (*F1*) and absorption rate constant (*ka*) equal the average *F1* and *ka* of the values in different preclinical species as determined in compartmental PK models (Vuppugalla *et al.*, 2011). As we described the PK of fingolimod and fingolimod-P only in rat, this yields the situation where the values of *F1* and *ka* are the same in rat and human.

Computation

Data from the *in vivo* and *ex vivo* studies were analyzed simultaneously using the non-linear mixed-effects modeling approach implemented in NONMEM (version 7.1.0; Icon Development Solutions, Ellicott City, Maryland, USA). The models were compiled using Digital Fortran (version 6.6C3, Compaq Computer Corporation, Houston, Texas) and executed on a PC equipped with an AMD Athlon 64 processor 3200+ under Windows XP. The results were analyzed using the statistical software package S-Plus for Windows (version 6.2 Professional, Insightful Corp., Seattle, USA). Parameters were estimated using the first order conditional estimation method with interaction between the two levels of stochastic effects (FOCE interaction). Random effects were included as exponential terms reflecting lognormal distributions of model parameters. The residual variability was explored with proportional and additive error models. Goodness-of-fit was determined using the minimum value of the objective function defined as minus twice the log-likelihood. For nested models, a decrease of 10.8 points in the minimum value of the objective function (MVOF) (corresponding to $p<0.001$ in a chi-squared distribution) by adding an additional parameter was considered significant. The goodness-of fit was also investigated by visual inspection of the plots of individual predictions and the diagnostic plots of (weighted) residuals. To evaluate the predictive value of the human pharmacokinetic model a visual predictive check (VPC) was performed in which the median and the 90% inter-quantile range of data simulated with the developed model were plotted together with the observations. In addition, the predictive value of the human pharmacokinetic model was externally validated with data from study 2215 using the same VPC technique.

Results

Rat PK model

The data from the rat *ex* and *in vivo* studies (studies 1 and 2) were described by the model depicted in Figure 1, (Rat). The phosphorylation of fingolimod was described by the combination of a first-order process in the platelets (*k67*) and a first-order phosphorylation process in plasma (*k34*), which is only relevant *in vivo*. *In vivo* dephosphorylation was found to be faster than the *ex vivo* dephosphorylation. This was accounted for by estimating an extra rate constant (*k43b*), which is only relevant *in vivo*. The disposition of fingolimod and fingolimod-P were characterized by three-compartmental models with saturable distribution from the plasma to one of the peripheral compartments for fingolimod and fingolimod-P. The absorption and elimination of fingolimod were described by first-order processes (*ka* and *k30*). Fingolimod was also pre-systemically phosphorylated. As calculated from the absorption rates, 82% of the total fingolimod dose was converted

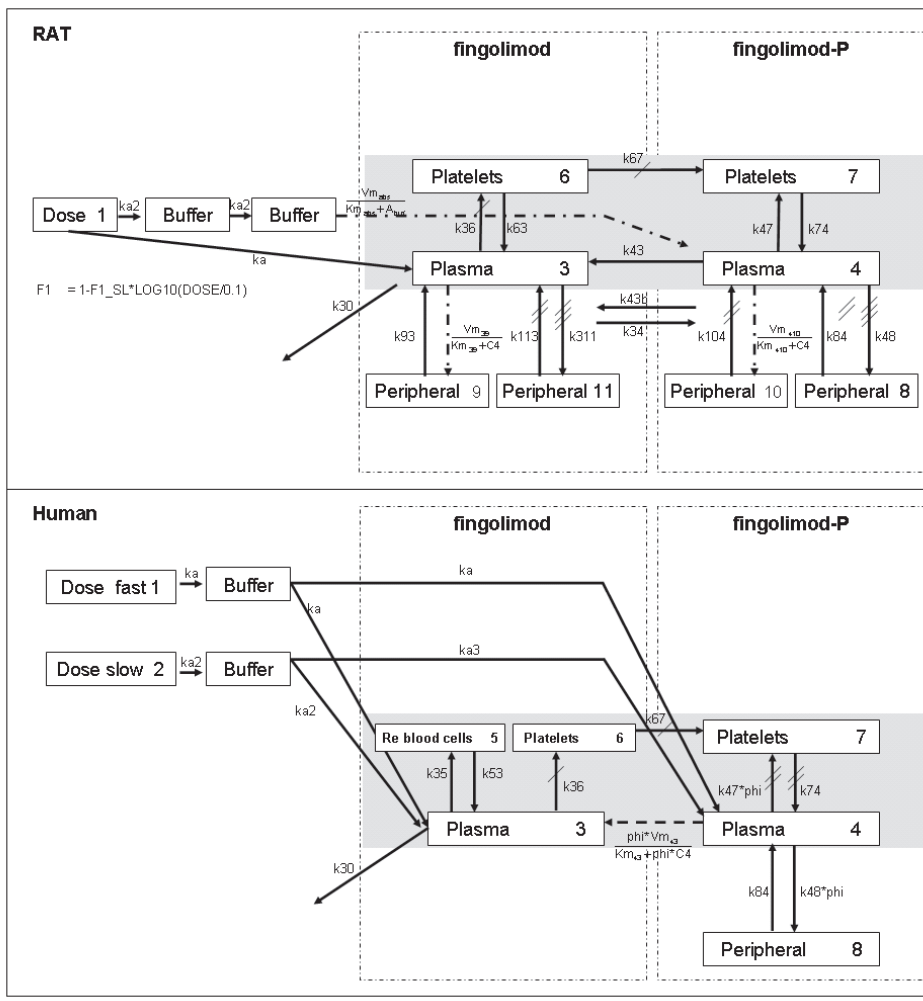

Figure 1: Pharmacokinetic models to describe the time course of the fingolimod and fingolimod-P blood concentration in rat and human.

The grey area describes the inter-conversion and blood/plasma distribution in isolated blood. Kxy represent the first-order distribution and elimination rate constants. Arrows with an equal number of slashes indicate that these rates are the same. In addition, the dashed lines represent saturable processes.

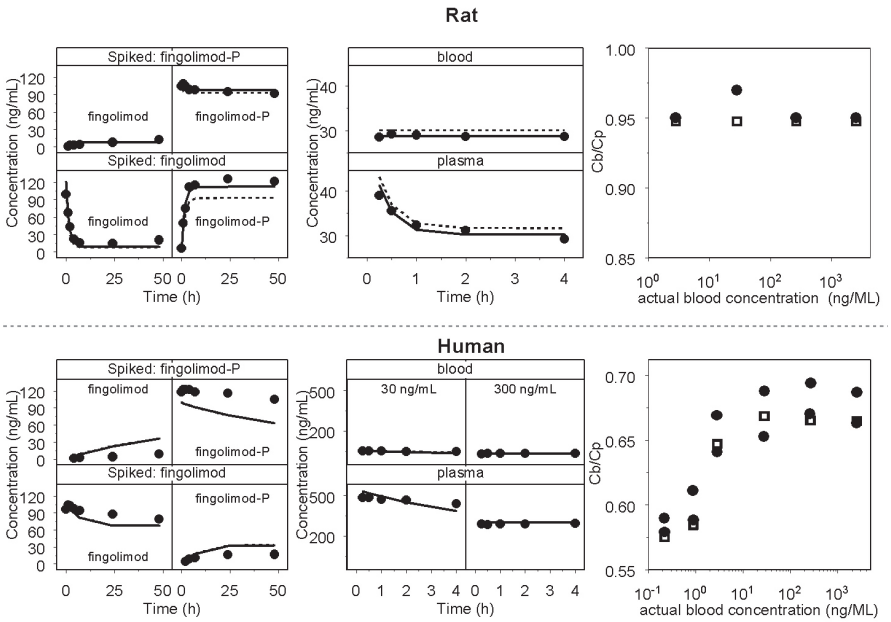

Figure 2: Description of the data from the *ex vivo* inter-conversion (A) and blood/plasma distribution (B and C) studies in isolated blood from rat (upper half) and human (lower half).
The dots represent the observations and the continuous lines (A and B) and squares (C) represent the individual predictions. The dashed lines represent the population predictions.

to fingolimod-P before entering the blood. The absorption of the pre-systemically formed fingolimod-P was characterized by two transit compartments to describe observed delay in absorption. In addition, the absorption from the last transit compartment to the central compartment was described by a saturable Michaelis-Menten like process. The bioavailability was found to decrease from 1, for a dose of 0.1 mg/kg, to 0.36, for the highest orally administered dose, i.e. 3 mg/kg, according to a descriptive log-dose equation (Table 2), which is only valid in the observed dose range between 0.1 and 3 mg/kg. The *ex-vivo* blood volume ($V_{ex\ vivo}$) and *in vivo* central volume of distribution ($V_{in\ vivo}$) were allowed to vary between experiments and between individual rats (IIV). The residual errors for the *ex* and *in vivo* were best described by proportional residual error models with an extra additive residual error for *ex vivo* experiment A.

The developed model adequately described the inter-conversion between fingolimod and fingolimod-P as well as the blood-plasma distribution as can be seen in the description

Table 2: The parameter values from the PK models to describe the time course of the fingolimod and fingolimod(-P) blood concentrations in rat and human

Parameter	Rat				Human			
	Value	*RSE*	*LLCI*	*ULCI*	*Value*	*RSE*	*LLCI*	*ULCI*
blood								
k67 (1/h)	2.61	19.1	1.63	3.59	0.151	17.0	0.101	0.201
k43 (1/h)	0.0870	14.4	0.0625	0.112	_			
VM_{43} (ng/(mL*h))	_				2.48	32.7	0.89	4.07
k36 (1/h)	fixed to k67				fixed to k67			
k63 (1/h)	5.90	45.8	0.608	11.2	_			
k35 (1/h)					0.195	21.2	0.114	0.276
k53 (1/h)					0.0328	12.7	0.0246	0.0410
k74 (1/h)	1.70	10.9	1.34	2.06	0.106	16.7	0.0713	0.141
k47 (fraction of k74)	0.773	1.68	0.748	0.798	1 fixed			
$KM4_3$ (ng/mL)	_				0.729	27.4	0.337	1.12
B_{max} (ng/mL)	_				3.79	16.8	2.54	5.04
Kd (ng/mL)	_				0.0795	23.0	0.0436	0.115
$V_{ex\text{-}vivo}$ (L)	1 fixed				1 fixed			
1-hematocrit	0.535 fixed				0.55 fixed			
disposition								
k30 (1/h)	3.67	12.2	2.79	4.55	0.104	12.6	0.0783	0.1297
$V_{in\text{-}vivo}$ (human: L; rat: L/kg)	0.211	11.0	0.166	0.256	475	8.44	396	554
k311 (1/h)	21.6	18.2	13.9	29.3	_			
k113 (1/h)	1.75	9.43	1.43	2.07	_			
k48 (1/h)	fixed to k311				fixed to VM_{43}			
k84 (1/h)	fixed to k113				0.0158	18.4	0.0101	0.0215
VM_{39} (ng/(mL*h))	3170	23.6	1706	4634	_			
k93 (1/h)	26.6	21.4	15.4	37.8	_			
KM_{39} (ng/mL)	43.0	30.0	17.7	68.3	_			
VM_{410} (ng/(mL*h))	fixed to VM39				_			
k104 (1/h)	fixed to k113				_			
k34std1 (1/h)	16.4	10.3	13.1	19.7	_			
k34std2 (1/h)	2.68	9.33	2.19	3.17	_			
k43b (1/h)	4.82	8.57	4.01	5.63	_			

Table 2 *Continued*

Parameter	Rat				Human			
absorption								
FRAC going to dose cmt1	_				0.356	8.46	0.297	0.415
$FRAC_{STD2105}$ going to dose cmt 1	_				0.283	12.8	0.212	0.354
ka (1/h)	0.114	14.7	0.0811	0.147	1.94	7.06	1.67	2.21
$ka_{STD2105}$ (1/h)					9 fixed			
ka2 (1/h)	0.534	12.6	0.402	0.666	0.402	13.2	0.298	0.506
$ka2_{STD2105}$ (1/h)	_				0.474	15.9	0.326	0.622
ka3 (1/h)	_				1.53	22.1	0.868	2.19
ALAG2 (h)					3.10	3.97	2.86	3.34
VM_{abs} (ng/h)	105	16.7	70.7	139	_			
KM_{abs} (ng)	10.6	40.1	2.27	18.9	_			
F1_SL	-0.430	4.21	-0.465	-0.395	_			
Inter-Individual variability								
$V_{ex\text{-}vivo}$ (CV%)	10.9		<0	16.8	_			
$V_{in\text{-}vivo}$ (CV%)	11.7		4.03	16.1	17.3	8.86	14.0	20.1
$K30_{in\text{-}vivo}$ (CV%)	_				38.6	9.71	30.6	45.5
Residual variability								
Prop. $Res.Error_{ex\text{-}vivo}$ (CV%)	2.40		1.67	2.96	57.9		33.9	77.3
Add. $Res.Error_{ex\text{-}vivoA}$ (CV%)	6.81		<0	9.91				
Prop. $Res.Error_{ex\text{-}vivoB}$ (CV%)	_				8.2		1.1	11.6
Prop. $Res.Error_{ex\text{-}vivoC}$ (CV%)	_				27.1		<0	46.6
Prop. $Res.Error_{fingolimod\_in\text{-}vivo}$ (CV%)	26.4		19.96	31.66	15.3		13.1	17.3
Prop. $Res.Error_{fingolimod\text{-}P\_in\text{-}vivo}$ (CV%)	24.3		20.89	27.34	23.4		20.0	26.4

RSE: Relative Standard Error

LLCI: Lower limit of 95 % confidence interval

ULCI: Upper limit of 95 % confidence interval

CV: Coefficient of variation

F1=1-F_SL*LOG10*(DOSE/0.1)

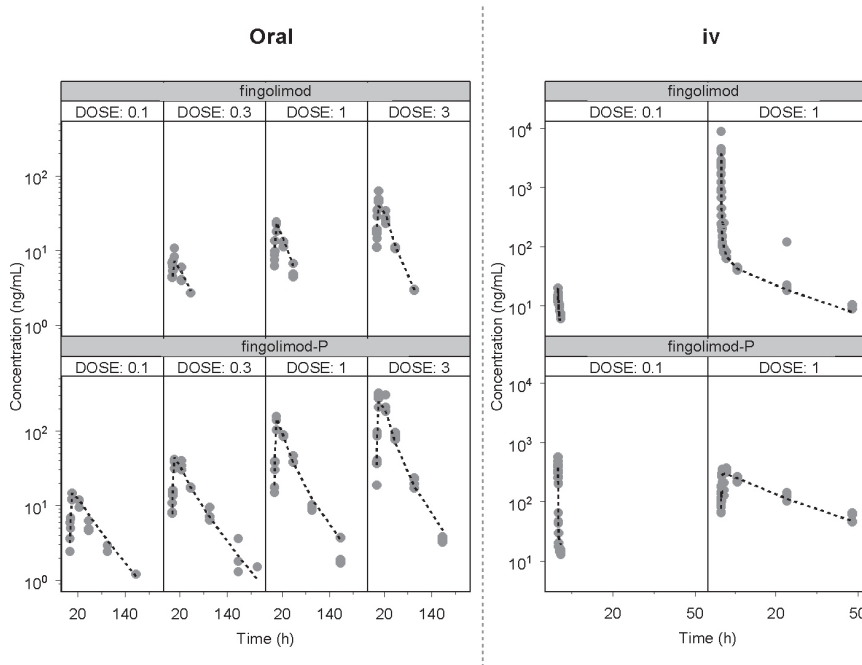

Figure 3: Description of the fingolimod and fingolimod-P blood concentrations from studies 1 and 2 after oral fingolimod (dose: 0.1, 0.3, 1, or 3 mg/kg) or intravenous administration of fingolimod (dose: 1 mg/kg) or fingolimod-P (dose: 0.1 mg/kg)

The grey dots represent the observations and the dashed lines represent the population predictions.

of the data from the *ex vivo* experiments (Figure 2, Rat). The *in vivo* time course of the fingolimod(-P) blood concentrations was also adequately described after both iv and oral administration of fingolimod (Figure 3). All parameters could be estimated with good precision as all standard errors were less than 50% of the parameter estimates (Table 2). The estimated clearance of 0.774 L/h/kg does not differ from the systemic clearance of 0.748 L/h/kg derived from a published physiologically based pharmacokinetic (PBPK) model (Meno-Tetang *et al.*, 2006).

Allometric scaling

The predicted PK of fingolimod and figolimod-P in human after allometric scaling demonstrated that the fingolimod exposure was adequately predicted, but the fingolimod-P exposure was 12-fold over-predicted (Figure 4). Hence, an allometric scaling approach seems not applicable for predicting fingolimod-P exposure in human.

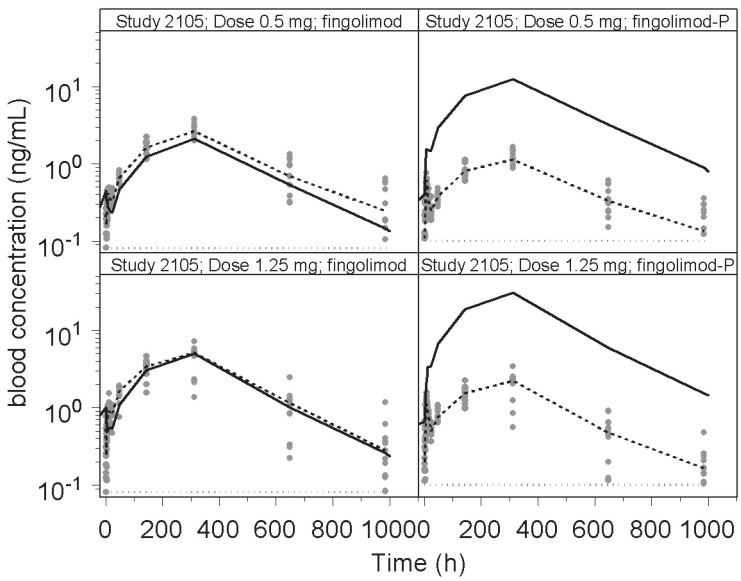

Figure 4: Prediction of the fingolimod and fingolimod-P blood concentrations from multiple dose studies 2105 in health volunteers using the allometrically scaled rat model

The grey dots represent the observations after administration of fingolimod (0.5 or 1.25 mg po) and the dashed lines represent the observed median. The continuous lines represent the predicted median.

Human PK model

The model to describe the data from the human *ex* and *in vivo* studies (studies 2213 and 2105) was comparable to the model to describe the rat data (Figure 1, Human). However, several differences are noticeable between the rat and human models. i) Only one peripheral compartment could be quantified to describe the distribution of fingolimod-P. ii) The phosphorylation and dephosphorylation processes in plasma, which were identified in rat, could not be quantified in human. Instead, the dephosphorylation in plasma was described by a saturable, Michaelis-Menten like process (Equation 1). iii) In human, two peaks were observed during the absorption phase. This was described by two dose compartments with a lag time for the absorption from the second dose compartment. iv) The distribution of fingolimod into the red blood cells could be quantified in human, whereas this process could not be quantified in rat. v) The distribution of fingolimod-P into the platelets and the peripheral compartment was found to be faster for higher concentrations. This was described by a saturable binding process (Equation 2) resulting in a higher blood/plasma

ratio for higher concentrations (Figure 2C, human). *k30* and the $V_{in\ vivo}$ were allowed to vary between individual subjects. The residual errors for the *ex* and *in vivo* studies were best described by proportional residual error models.

In general, the developed model adequately described the data from the *ex vivo* studies (Figure 2, Human). In addition, the time course of the *in vivo* fingolimod and fingolimod-P blood concentrations was adequately described as the continuous lines, which represent the predicted median, closely resemble the observed median (dashed lines) (Figure 5). However, the observations from the 1.25 mg dose group in study 2105 were slightly over-predicted. For study 2213, the variability was adequately predicted as about 90% of the observations are within the 90% prediction interval (grey area) (Figure 5). For study 2105, the variability was slightly over-predicted. All parameters could be estimated with good precision as all standard errors were less than 50% of the parameter estimates (Table 2).

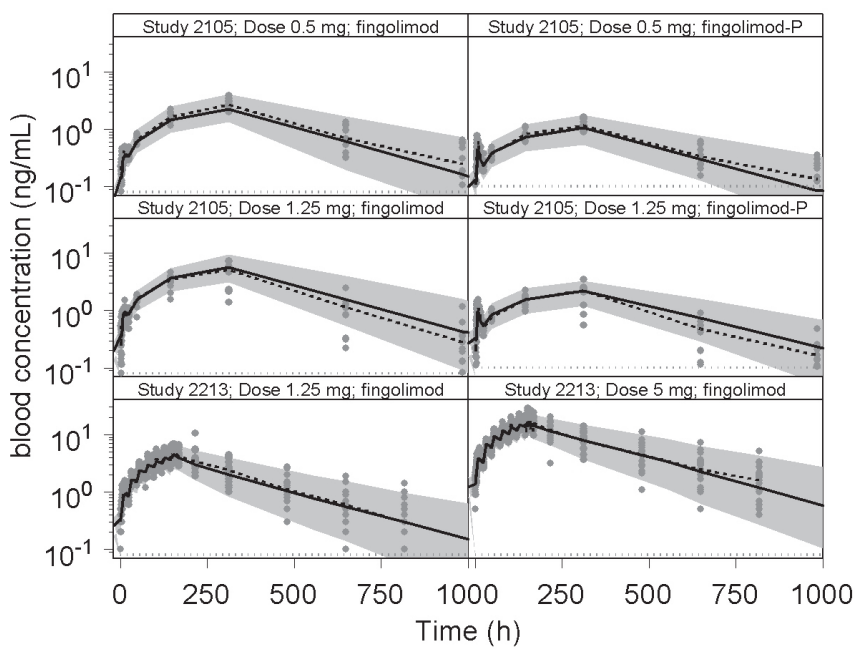

Figure 5: Visual predictive check of the description of the fingolimod and fingolimod-P blood concentrations from multiple dose studies 2105 and 2213 in health volunteers

The grey dots represent the observations after administration of fingolimod (0.5, 1.25 or 5 mg po) and the dashed lines represent the observed median. The continuous lines represent the predicted median and the grey area represents the 90% prediction interval.

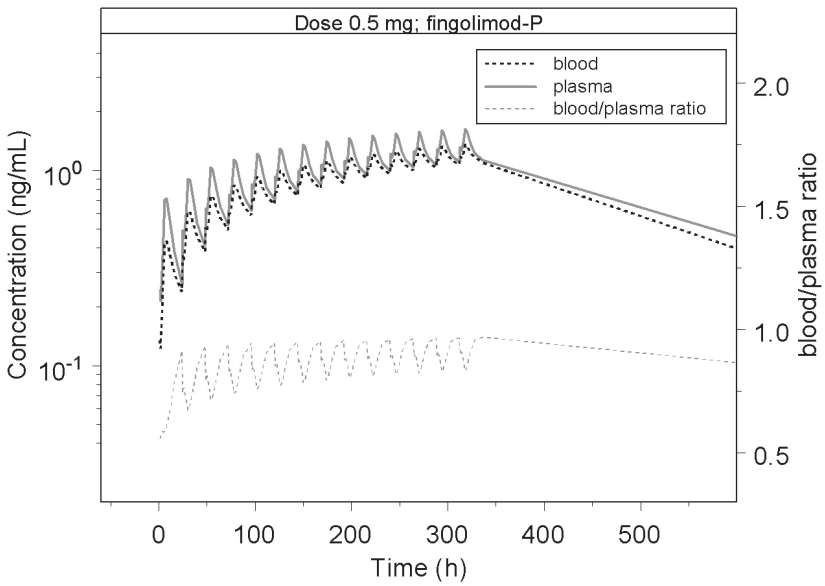

Figure 6: Predicted fingolimod-P blood and plasma concentrations and blood/plasma ratio after once daily administration of fingolimod during 14 days

The grey line represents the predicted fingolimod-P plasma concentration and the dashed lines black represents the predicted fingolimod-P blood concentration after administration of fingolimod (0.5 mg po). The dashed grey line represents the predicted blood/plasma ratio.

About 69% of the total fingolimod dose was converted to fingolimod-P before entering the blood. A comparison of the time course of the predicted fingolimod-P blood and plasma concentrations demonstrates that for a dose of 0.5 mg/day the fingolimod-P blood/plasma concentration ratio varies between 0.8 and 0.95 within a day at steady state. The difference between blood and plasma concentrations is the largest around t_{max} (Figure 6). The developed model could, in general, adequately predict both the trend and the variability in the data from the external (i.e. study not used for model development) study 2215 (Figure 7). However, fingolimod and fingolimod-P concentrations observed in the 10 mg dose-group were slightly over-predicted. On the other hand the concentrations of 5 out of 6 subjects included in this treatment-group fall within the prediction interval. Therefore, this might be a chance observation, which is due to the low number of subjects. The observed concentrations of the 6^{th} subject of this treatment are much lower than predicted, but also much lower than the observed concentrations in the lowest dose group. In addition, the maximum fingolimod-P concentrations are slightly under-predicted for the higher dose groups. This indicates that there might be another non-linear process involved that becomes relevant after administration of doses higher than 10 mg.

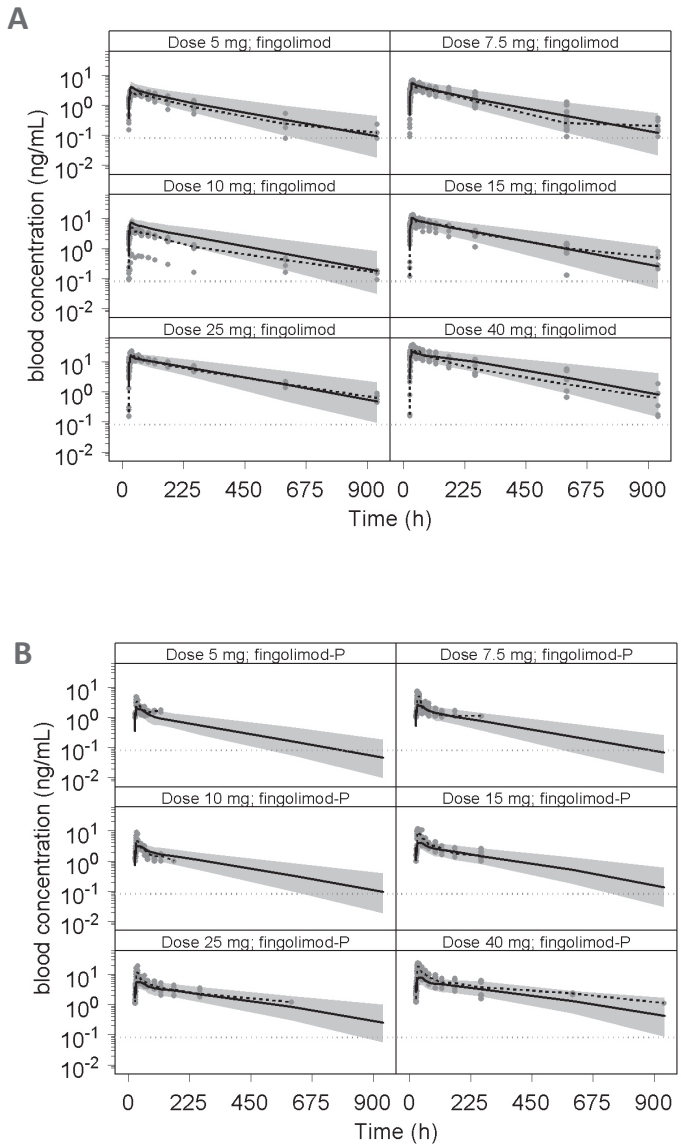

Figure 7: Prediction of the fingolimod and fingolimod-P blood concentrations from single dose study 2215 in health volunteers

The grey dots represent the observations after administration of fingolimod (5-40 mg po) and the dashed lines represent the observed median. The continuous lines represent the predicted median and the grey area represents the 90% prediction interval.

Comparison of exposure between rat and human

A comparison between the predicted steady-state fingolimod-P exposure in rat and human demonstrated that fingolimod-P exposure was about 10-12 fold lower in human as compared to rat for equivalent doses when following a dose-by-factor approach, which is commonly applied to scale the 'no-observed adverse effect level' (Figure 8)(Sharma and McNeill, 2009; FDA, 2010). This approach uses allometric scaling on the basis of body surface area. Generally, an exponent of 0.67 or 0.75 is used. For example, in rat a dose of 0.1 mg/kg results in an exposure of 1005 ng*h/mL. The human-equivalent dose after applying the dose-by-factor approach with an exponent of 0.75 equals 1.8 mg ($0.1*70*(70/0.3)^{-0.25}$). The "observed" exposure as predicted by the developed PK model for human was 95 ng*h/mL. As a result, there was an 11 (1005/95) fold difference in exposure between rat and human.

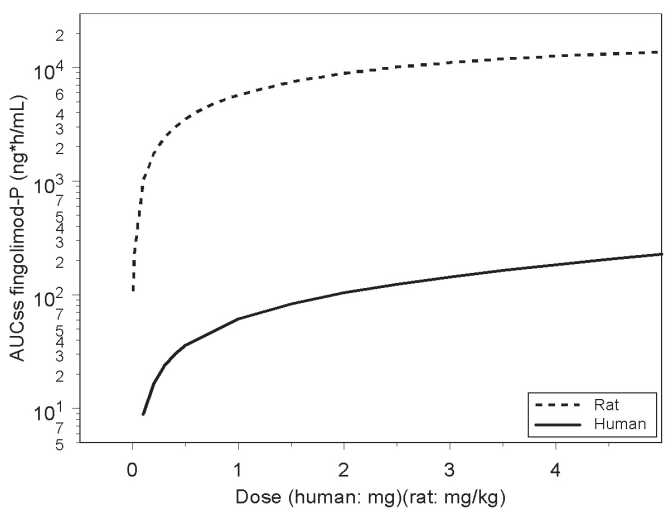

Figure 8: Comparison of the predicted steady state fingolimod-P exposures in blood after oral administration of fingolimod in doses of 0.1-5 mg/kg in rat and 0.1-5 mg in human.
The dashed and continuous lines represent the exposure in rat and human, respectively.

Discussion

With the aim of 1) of investigating whether characterization of the phosphorylation in blood platelets constitutes a basis for pharmacokinetic scaling and 2) predicting plasma rather than whole blood concentrations of fingolimod phosphate, PK models were de-

veloped to quantify the exposure of the prototypical S1PHK substrate fingolimod and its active metabolite, fingolimod-P, in rat and human. Previously, the time course of the blood concentrations of the parent compound but not the phosphorylated metabolite has been described by a physiologically-based pharmacokinetic model (Meno-Tetang *et al.*, 2006). In addition, the time course of the fingolimod-P blood concentrations has been described by a descriptive population PK model (Wu *et al.*, 2011). However, to date, no pharmacokinetic models have been published that describe the time course of the fingolimod and fingolimod-P concentrations simultaneously.

The developed models, i.e. the rat model and the human model, consisted of three parts to describe the phosphorylation and the dephosphorylation in blood, the distribution and elimination from the systemic circulations and the absorption, respectively. Although both models were structurally related, several differences are noticeable between the rat and human models. First of all, not all peripheral compartments that were identified in the rat model could be identified in the human model. This is explained by the fact that fingolimod(-P) concentrations were not measured following intravenous administration of fingolimod in human, and therefore, less detailed information was available about the distribution. Another important difference between the rat and human model is that saturable binding to a high affinity/low capacity binding site on a protein in the plasma was identified in humans, whereas this could not be identified in rats. As a result, the fingolimod-P blood/plasma exposure ratio was constant over the observed dose range (the ratio was about 1) in rats, whereas this ratio increased with higher doses from 0.95 for a dose of 0.5 mg to 1.9 for a dose of 5 mg at steady state in human. Therefore, the human plasma concentrations may be a little higher than anticipated after administration of doses below 0.5 mg/day. In addition, for a dose of 0.5 mg/day the blood/plasma concentration ratio varied between 0.8 and 0.95 within a day at steady state (Figure 6). The difference between blood and plasma concentrations is the largest around $t_{max.}$ This is relevant since the fingolimod-P plasma concentrations are likely to be more predictive for pharmacodynamic effects than blood concentrations. Finally, in both species, the *in vivo* dephosphorylation was found to be much faster than the dephosphorylation in isolated blood. Fingolimod-P is dephosphorylated by LLP3, which is expressed on cells exposed to plasma such as vascular endothelial cells, which are not present in the isolated blood used for the *ex vivo* studies. In humans, dephosphorylation is best described by a Michaelis-Menten process, whereas in rats no capacity limited (Michelis-Menten) kinetics could be identified, due to the limited concentration range that has been studied. The developed models are valid in the evaluated dose range of 0.1 to 3 mg/kg following oral administration in rat and 0.5 to 5 mg following oral once daily administration to humans. In general, the data from the studies in rat and human were adequately described. However, in study

2105 the observations from the 1.25 mg dose group were slightly over-predicted. This is thought to be due to non-compliance for some subjects in this treatment group. In addition, for this study, the variability was slightly over-predicted. As there were only 12 subjects per treatment-group included in this study the observed variability may not be representative for the variability in a larger population. An external validation of the human model using data from a single-dose study with doses between 5 and 40 mg demonstrated that the model can also be used to predict fingolimod(-P) blood concentrations following doses up to 10 mg, which is a dose well above the therapeutic dose of 0.5 mg once daily. The developed models can be applied to evaluate possible covariate influences or to predict the time course of the fingolimod and fingolimod-P plasma concentrations. Moreover, the model can be applied to characterize the time course of pharmacodynamic effects of fingolimod-P by linking the time course of the fingolimod-P plasma or blood concentrations to pharmacodynamic observations.

Besides describing the PK of fingolimod and fingolimod-P in human by a compartmental model, the PK in human were predicted from rat data using an allometric scaling approach. Various dose extrapolation techniques have been described ranging from empirical allometric scaling to semi-mechanistic methodologies, which attempt to account for species difference in physiology, and further to the mechanistic whole-body PBPK modeling approach, which relies on physicochemical properties of the drug and knowledge of human physiology (tissue composition)(Jones et al, 2011). Allometric scaling of the PK parameters from rat resulted in an adequate prediction of the PK of fingolimod. However, the exposure of fingolimod-P was 12-fold over-predicted. When examining the inter-conversion rate parameters in both species it is noticeable that the phosphorylation of fingolimod in the platelets is 4-fold faster in rats as compared to humans after allometric scaling (Table 1, *K67*). As in rats, an extra phosphorylation rate was estimated in the plasma, the overall phosphorylation was 9-fold faster in rats as compared to humans. This extra phosphorylation could represent rapid phosphorylation in other tissues, but this rate was not quantifiable in human. This could possibly be due to differences in the S1PHK2 enzyme tissue distribution, which may also explain the inadequate allometric prediction of the volume of distribution as inter-species differences in inter-conversion are not accounted for in a general allometric scaling approach. Overall, the 4-fold difference in phosphorylation rate quantified from the *ex vivo* experiments is indicative for differences in exposure between rat and human, but does not exclusively elucidate this difference. This is explained by the minor contribution of phosporylation in the platelets as compared to the 82% and 69% pre-systemic phosphorylation seen in rats and humans, respectively. More mechanistic approaches are required to integrate the differences in pre-systemic

phosphorylation and enzyme tissue distribution in the translational pharmacokinetics of fingolimod and fingolimod-P and other S1PHK substrates.

In conclusion, large interspecies differences in the rate of phosphorylation between rats and humans were demonstrated, using fingolimod as a paradigm compound, which cannot be accounted for by allometric scaling. A semi-mechanistic PK model is proposed that constitutes a basis for the prediction of the concentrations of S1PHK substrates and their phosphorylated metabolites in plasma. In this model, differences in the rate of phosphorylation in blood, estimated from *ex vivo* inter-conversion measurements in platelets, partly explain the differences in exposure between rats and humans. However, differences in pre-systemic phosphorylation should also be taken into account.

References

Albert R, Hinterding K, Brinkmann V, Guerini D, Muller-Hartwieg C, Knecht H, et al. (2005). Novel immunomodulator FTY720 is phosphorylated in rats and humans to form a single stereoisomer. Identification, chemical proof, and biological characterization of the biologically active species and its enantiomer. *J Med Chem.*, 48, 5373-5377.

Anada Y, Igarashi Y & Kihara A (2007). The immunomodulator FTY720 is phosphorylated and released from platelets. *Eur J Pharmacol.,* 568, 106-111.

Billich A, Bornancin F, Devay P, Mechtcheriakova D, Urtz N & Baumruker T (2003). Phosphorylation of the immunomodulatory drug FTY720 by sphingosine kinases. *J Biol Chem., 278*, 47408-47415.

Brinkmann V (2007). Sphingosine 1-phosphate receptors in health and disease: mechanistic insights from gene deletion studies and reverse pharmacology. *Pharmacol Ther.,* 115, 84-105.

Brinkmann V, Cyster JG & Hla T (2004). FTY720: sphingosine 1-phosphate receptor-1 in the control of lymphocyte egress and endothelial barrier function. *Am J Transplant.*, 4, 1019-1025.

Chun J & Hartung HP (2010). Mechanism of action of oral fingolimod (FTY720) in multiple sclerosis. *Clin Neuropharmacol.*, 33, 91-101.

Cohen JA, Barkhof F, Comi G, Hartung HP, Khatri BO, Montalban X, et al. (2010). Oral fingolimod or intramuscular interferon for relapsing multiple sclerosis. *N Engl J Med.*, 362, 402-415.

Cusack KP & Stoffel RH (2010). S1P(1) receptor agonists: Assessment of selectivity and current clinical activity. Curr Opin Drug Discov Devel., 13, 481-488.

Danhof M, de Lange EC, Della Pasqua OE, Ploeger BA & Voskuyl RA (2008). Mechanism-based pharmacokinetic-pharmacodynamic (PK-PD) modeling in translational drug research. *Trends Pharmacol Sci.*, 29, 186-191.

FDA press release on approval of Gilenya (2010). Available at: http://www.fda.gov/NewsEvents/Newsroom/PressAnnouncements/ucm226755.htm (Accessed: 30 September 2012).

Hale JJ, Yan L, Neway WE, Hajdu R, Bergstrom JD, Milligan JA, et al. (2004). Synthesis, stereochemical determination and biochemical characterization of the enantiomeric phosphate esters of the novel immunosuppressive agent FTY720. *Bioorg Med Chem.*, 12, 4803-4807.

Jones RD, Jones HM, Rowland M, Gibson CR, Yates JW, Chien JY, et al. (2011). PhRMA CPCDC initiative on predictive models of human pharmacokinetics, part 2: Comparative assessment of prediction methods of human volume of distribution. *J Pharm Sci*, 30, 22553.

Kharel Y, Lee S, Snyder AH, Sheasley-O'neill S L, Morris MA, Setiady Y, et al. (2005). Sphingosine kinase 2 is required for modulation of lymphocyte traffic by FTY720. *J Biol Chem.*, 280, 36865-36872.

Kihara A & Igarashi Y (2008). Production and release of sphingosine 1-phosphate and the phosphorylated form of the immunomodulator FTY720. *Biochim Biophys Acta.*, 1781, 496-502.

Kovarik JM, Hartmann S, Bartlett M, Riviere GJ, Neddermann D, Wang Y, et al. (2007). Oral-intravenous crossover study of fingolimod pharmacokinetics, lymphocyte responses and cardiac effects. *Biopharm Drug Dispos*., 28, 97-104.

Kovarik JM, Schmouder R, Barilla D, Wang Y & Kraus G (2004). Single-dose FTY720 pharmacokinetics, food effect, and pharmacological responses in healthy subjects. *Br J Clin Pharmacol.*, 57, 586-591.

Liu H, Sugiura M, Nava VE, Edsall LC, Kono K, Poulton S, et al. (2000). Molecular cloning and functional characterization of a novel mammalian sphingosine kinase type 2 isoform. *J Biol Chem.*, 275, 19513-19520.

Mandala S, Hajdu R, Bergstrom J, Quackenbush E, Xie J, Milligan J, et al.(2002). Alteration of lymphocyte trafficking by sphingosine-1-phosphate receptor agonists. *Science.*, 296, 346-349.

Meno-Tetang GM, Li H, Mis S, Pyszczynski N, Heining P, Lowe P & Jusko WJ (2006). Physiologically based pharmacokinetic modeling of FTY720 (2-amino-2[2-(-4-octylphenyl)ethyl]propane-1,3-diol hydrochloride) in rats after oral and intravenous doses. *Drug Metab Dispos.*, 34, 1480-1487.

Olivera A, Kohama T, Tu Z, Milstien S & Spiegel S (1998). Purification and characterization of rat kidney sphingosine kinase. *J Biol Chem.*, 273, 12576-12583.

Paugh SW, Payne SG, Barbour SE, Milstien S & Spiegel S (2003). The immunosuppressant FTY720 is

phosphorylated by sphingosine kinase type 2. *FEBS Lett.*, 554, 189-193.

Sharma V & McNeill JH (2009). To scale or not to scale: the principles of dose extrapolation. *Br J Pharmacol.*, 157, 907-921.

Vuppugalla R, Marathe P, He H, Jones RD, Yates JW, Jones HM, et al. (2011). PhRMA CPCDC initiative on predictive models of human pharmacokinetics, part 4: Prediction of plasma concentration-time profiles in human from in vivo preclinical data by using the Wajima approach. *J Pharm Sci*, 7, 22551.

West GB, Brown JH & Enquist BJ (1999). The fourth dimension of life: fractal geometry and allometric scaling of organisms. *Science.*, 284, 1677-1679.

Wu K, Mercier F, David OJ, Schmouder RL & Looby M (2011). Population Pharmacokinetics of Fingolimod Phosphate in Healthy Participants. *J Clin Pharmacol*, 22, 22.

Zollinger M, Gschwind HP, Jin Y, Sayer C, Zecri F & Hartmann S (2011). Absorption and disposition of the sphingosine 1-phosphate receptor modulator fingolimod (FTY720) in healthy volunteers: a case of xenobiotic biotransformation following endogenous metabolic pathways. *Drug Metab Dispos.*, 39, 199-207.

Abbreviations

B_{max}	Binding capacity
F1	Bioavailability
fingolimod-P	Fingolimod-phosphate
IIV	Inter-individual variability
iv	Intravenous
ka	Absorption rate constant
Kd	Binding affinity
Km	Concentration at which the half maximal rate of biotransformation is reached
kxx	First order rate constant
LLP3	Lipid phosphatase type 3
LOQ	Lower limits of quantification
MVOF	Minimum value of the objective function
PBPK	Physiologically based pharmacokinetic
PD	Pharmacodynamic
PK	Pharmacokinetic
S1P	Sphingosine 1-phosphate
S1PHK	Sphingosine kinase
$V_{ex\ vivo}$	*Ex-vivo* blood volume
$V_{in\ vivo}$	*In-vivo* blood volume
Vm	Maximum rate of biotransformation
VPC	Visual predictive check